IEICE TRANSACTIONS

on Electronics

This advance publication article will be replaced by the finalized version after proofreading.

BRIEF PAPER

Voltage-Current Characteristics for Each Arc Length of Break Arcs Generated in a 48VDC/50A-600A Resistive Circuit

Keiya IMORI[†a)], *Student member* and Junya SEKIKAWA[†b)], *member*

SUMMARY Electrical contacts are separated at a constant opening speed in a 48VDC/50A-600A resistive circuit. Break arcs are observed using two high-speed cameras from the top and side directions. Lengths of the break arcs are analyzed from images taken by the cameras. Arc voltages and currents corresponding to the analyzed arc lengths are investigated to obtain voltage-current characteristics of the break arcs. Relationships between the arc length versus gap voltage and the arc length versus circuit current are obtained. These results are slightly scattered. Therefore, to obtain one-to-one relationships between the arc length and the gap voltage, approximate curves should be determined for these results. Using these approximate curves, eventually, the voltage-current characteristics for each arc length are indicated.
key words: Electro-magnetic relay, High-speed camera, Arc discharge, Electrical contacts.

1. Introduction

The electrification of power units is progressing rapidly as a means of improving the fuel efficiency of vehicles. There are fully electrified electric vehicles and hybrid vehicles equipped with both internal combustion engines and electric motors. Among hybrid vehicles, mild hybrid systems use small electric motors to improve fuel efficiency at low cost. Many 48VDC systems have been adopted for the vehicle systems [1]. Large currents of hundreds of amperes are used in these systems, and related devices such as electro-magnetic relays and connectors have been developed for these systems.

When DC circuits are interrupted by electrical contacts mounted on electromagnetic relays, break arcs occur between the contacts [2]. For DC circuits with resistive loads, the break arcs are extinguished when the arc voltage reaches a supply voltage. In other words, it is important to quickly increase the arc voltage to the supply voltage for arc extinction to reduce damage to electrical contacts mounted on these devices. Therefore, characteristics of break arcs are investigated by many researchers [3-14].

Arc voltage-current characteristics for each arc length are known as the fundamental characteristic of break arcs [15]. If the voltage-current characteristics are available within the range of voltage and current of the circuit in which the

electrical contacts are used, the characteristics of the arc voltage to the current, and the arc length at extinction with using load lines can be determined [15]. The authors reported voltage-current characteristics for a 54VDC/10A resistive circuit with Au, Ag, Cu, Pt and Ni contact pairs [12]. The arc length and duration for 300VDC/300A resistive circuits ware investigated by the authors [13, 14]. Many voltage-current characteristics for various arc discharges are shown in a literature [16]. However, there are few voltage-current characteristics especially for arc voltages of several tens of volts and currents of hundreds of amperes. In other words, the voltage-current characteristics in these voltage and current ranges are unknown.

In this paper, therefore, the voltage-current characteristics of break arcs generated in a 48VDC/50A-600A resistive circuit are investigated. The break arcs are generated between silver electrical contacts and observed by high-speed cameras. Arc lengths are analyzed using observed images. The characteristics for each arc length of the break arcs are shown.

2. Experimental and Analysis Methods

An experimental equipment, experimental conditions, and analysis methods are described in this chapter.

2.1 Experimental Equipment

Figure 1 shows an experimental circuit. The circuit consists of a DC power supply E, a charge current limiting resistor R_1, a capacitor C, a switch S, a load resistor R_2, a pair of horizontally opposed electrical contacts, a current measuring resistor R_3 and a resistor R_4. The R_1 is 2Ω. The R_2 is variable ranging from 0.08 Ω to 1 Ω. The capacitor C is
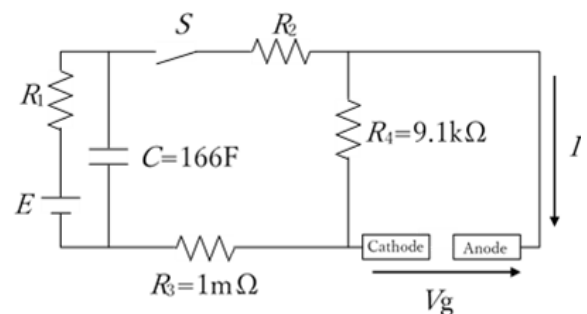

Fig. 1 Experimental circuit.

†The authors are with the Graduate School of Engineering, Shizuoka University, Hamamatsu-shi, 432-8561 Japan.
a) E-mail: imori.keiya.18@shizuoka.ac.jp
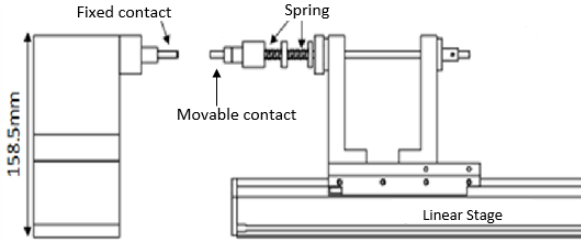b) E-mail: sekikawa.junya@shizuoka.ac.jp

Fig. 2 Schematic of contact separating device

an electric double layer capacitor. The resistor R_4 is used to stabilize the anode potential when the switch S and the contacts are turned off. The circuit operation during an experimental operation is explained below. The capacitor C is fully charged by the power supply E. After the contacts are brought into contact, the switch S is turned on and the current flows through the capacitor C, the resistor R_2, the contacts, and the resistor R_3 loop. Immediately after that energizing, the contacts are separated, and a break arc is generated between the contacts.

The voltage between the contacts is V_g and the circuit current is I. The current when the contacts are contacted is defined as I_0.

A schematic of a contact separating device is shown in Fig. 2. A movable contact is contacted to a fixed contact, then the current flows through the contacts, and the movable contact is separated by a linear stage at constant opening speed v. The cathode is fixed, and the anode is movable.

The contacts are cylindrical rods with a diameter of 5 mm.

Table 1 Experimental conditions

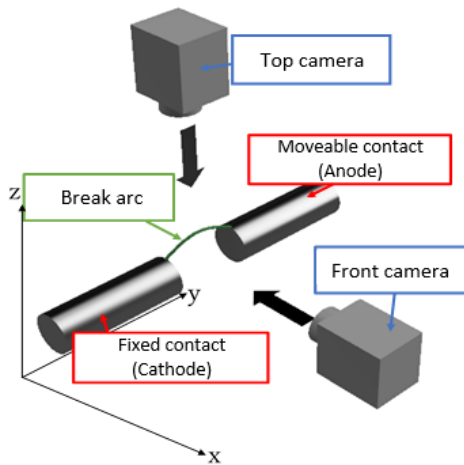| Supply voltage E[V]	48
Circuit current when contacts are contacted I_0[A]	50,100,200,300,400,500,600
Contact opening speed v[m/s]	0.5
Contact material	Ag99.99%
Atmosphere	Air

Fig. 3 Arrangement of electrical contacts and high-speed cameras

Table 2 High-speed camera settings

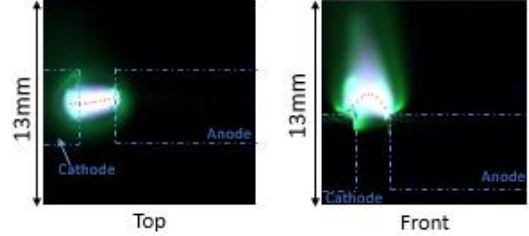| Frame rate [fps]	20000
Exposure time [μs]	2.0
Resolution [pixel]	256×256

Fig. 4 An example of images of a break arc (I_0=300A)

After polishing contact surfaces, the contacts were ultrasonically cleaned in ethanol and pure water for five minutes each. The fixed cathode surface is flat, and the movable anode surface is slightly curved.

2.2 Experimental Conditions

Table 1 shows experimental conditions. The number of break operations is five for each circuit current I_0. The contacts are polished and cleaned before break operations for each circuit current I_0.

The arrangement of the contacts and the high-speed cameras is shown in Fig. 3. Break arcs are observed simultaneously using two high-speed cameras (FASTCAM miniAX50) mounted horizontally and vertically. The voltage V_g between the contacts, the circuit current I are measured with a USB oscilloscope (Pico Scope 6). Table 2 shows settings of the high-speed cameras.
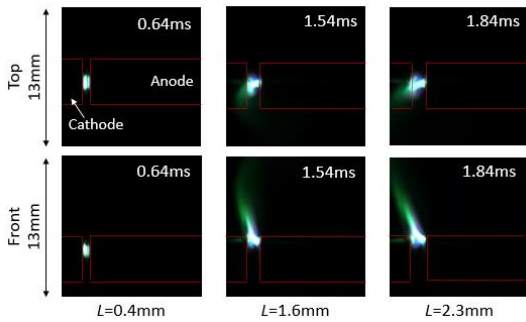
2.3 Analysis Methods

An example of images of a break arc is shown in Fig. 4 to explain an analysis method of arc length L. The top and front images were taken by the top and front cameras shown in Fig. 3, respectively. A path of the break arc is indicated as red plots in Fig. 4. These plots indicate center positions of width of the break arc along the current path direction. The arc length L is determined three-dimensionally as the path length.

3. Experimental and Analysis Results

In this chapter, an example of a break arc, approximations of the experimental and analysis results, and voltage-current characteristics are presented.

20220112 48V500A1
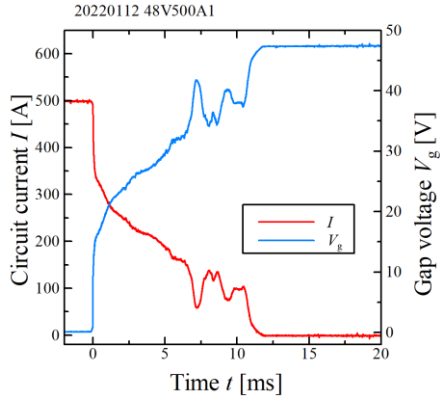
(a) Voltage and current waveforms

(b) Images of a break arc

Fig. 5 An example of a break arc
(First break operation at I_0=500A)

Fig. 6 Arc length – gap voltage characteristics (I_0=500A)

$L=-3.625 \times 10^{-3}V_g^2 +0.743V_g-13.033$

$L=2.998 \times 10^{-3}e^{0.285V_g}$

Fig. 7 Arc length – circuit current characteristics (I_0=500A)

$L=-3.005 \times 10^{-5}V_g^2 -0.038V_g+13.980$

$L=5.427 \times 10^{-2}e^{-0.022V_g}$

Fig. 8 Voltage-current characteristics for each arc length

3.1 An Example of a Break Arc

Fig. 5 shows the voltage and current waveforms and observed images of a break arc. The break arc is generated in the first break operation at I_0 = 500 A. As shown in Fig. 5(b), the break arc is generated near the center axis of the contacts, then moves upwards, and extinguishes. The cathode and anode spots reach to the top of the contact gap as shown in the front image of Fig. 5(b) at t=1.54ms. After that, as shown in images of Fig. 5(b) at t =1.84ms, the break arc extends upwards more clearly. This tendency was observed for all I_0 conditions.

3.2 Fittings of Analyzed Results

Figures 6 and 7 show the arc length-gap voltage and the arc length-circuit current characteristics at I_0=500A, respectively. Approximately 150 analyzed results for five break operations are indicated as plots in each figure. These plots are slightly scattered. Therefore, in order to obtain one-to-one relationships between the arc length L and the gap voltage V_g, approximate curves should be determined for these plots.

As described in previous section, the break arc extended upwards between the contact gap after the break arc reached
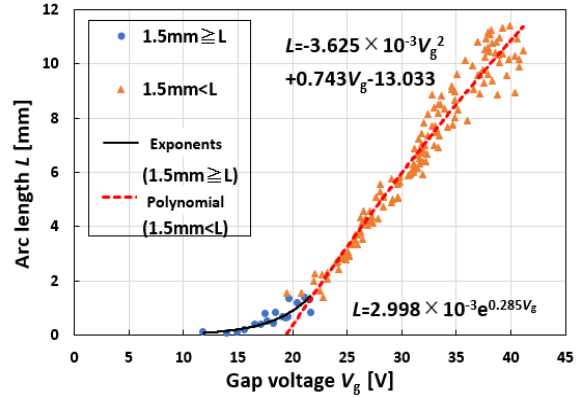
to the top of the contact gap. The arc length L at that time was about 1.6mm. As shown in Fig. 6, the tendency of the arc length L versus the gap voltage V_g changes at around L=1.5mm. This tendency may be caused due to the motion of the break arc described above. Therefore, the arc length of 1.5 mm was set as a boundary length for switching the approximate curves. In cases of Figs. 6 and 7 (I_0=500A),

exponential curves are applied when the L is smaller than 1.5mm, and polynomial curves are applied when the L is larger than or equal to 1.5 mm. These fittings are also applied to analyzed results for other I_0.

As shown in Fig. 6, when the L exceeds 8mm, i.e., when the V_g exceeds 35V, the plots tend to scatter and deviate from the approximate curve. This is because, as shown in Fig. 5(a), when the V_g exceeds 35V, the variation in the V_g becomes large, which causes the scattering in the L to increase. Same tendency is indicated for the L–I characteristics as shown in Fig. 7. To confirm the accuracy of approximate curves in Figs. 6 and 7, when the L is larger or equal to 1.5mm, the coefficients of determination (R^2) are calculated, and are 0.95 and 0.94, respectively. This result shows that the accuracy of the approximate curves is almost sufficient.

3.3 Voltage-Current Characteristics

Voltage – current characteristics of the break arcs for each arc length L is shown in Fig. 8. Each plot is calculated using the approximate curves for each I_0. As shown in Fig. 8, the characteristics are successfully obtained. When the current I is smaller than 200A, the characteristics are negative, and when the current I is larger than 200A, it is positive.

4. Conclusion

Electrical contacts were separated at constant opening speed in the 48VDC/50A-600A resistive circuit. The arc length was analyzed three-dimensionally using two high-speed cameras. Relationships between the arc length versus gap voltage and the arc length versus circuit current were obtained. Then, approximate curves for these relationships were determined. And using these curves, the voltage-current characteristics for each arc length were successfully obtained.

References

[1] T. Hayashi, "Can the 48V system see a revival?," in Nikkei Automotive Technology, January issue, pp.68-73, Tokyo, 2014.

[2] P. G. Slade, Electrical Contacts: Principles and Applications, Second Edition, pp.553-616, CRC Press, 2014.

[3] Y. Kayano, K. Miyanaga, H. Inoue, "Experimental Study on Arc Motion and Voltage Fluctuation at Slowly Separating Contact with External DC Magnetic Field," IEICE Trans. Electron., Vol. E97-C, No.9, pp.858-862, Sept. 2014.

[4] M. Hasegawa, "Influences of Contact Opening Speeds on Break Arc Behaviors of AgSnO₂ Contact Pairs in DC Inductive Load Conditions," IEICE Trans. Electron., Vol. E98-C, No.9, pp.923-927, Sept. 2015.

[5] S. Tokumitsu, M. Hasegawa, "Relationships between Break Arc Behaviors of AgSnO₂ Contacts and Lorentz Force to be Applied by an External Magnetic Force in a DC Inductive Load Circuit Up to 20V-17A," IEICE Trans. Electron., Vol. E102-C, No.9, pp.641-645, Sept. 2019.

[6] M. Hasegawa, S. Tokumitsu, "Influences of Contact Opening Speeds up to 200 mm/s and External Magnetic Field Application on Break Arc Duration Characteristics of AgSnO₂ Contacts in DC14V Load Conditions up to Around 10A," IEEE Trans. CPMT, Vol.8, No.3, March 2018.

[7] K. Yoshida, K. Sawa, K. Suzuki, M. Watanabe, "Influence of Arc Discharge on Contact Resistance of AgNi Contacts for Electromagnetic Contactors," IEICE Trans. Electron., Vol. E95-C, No.9, pp.1531-1534, Sept. 2012.

[8] K. Yoshida, K. Sawa, K. Suzuki, K. Takaya, "Influence of Contact Materials and Opening Velocity on Various Characteristics of DC High Voltage Arc," Proc. 63rd IEEE Holm Conf. on Electrical Contacts, pp.209-214, Sept. 2017.

[9] K. Sawa, M. Tsuruoka, and M. Morii, "Fundamental Characteristics of Arc Extinction at DC Low Current Interruption with High Voltage (<500V)," IEICE Trans. Electron., vol. E99-C, no.9, pp.1016–1022, Sept. 2016.

[10] K.Sawa, K.Yoshida, K.Suzuki, "Influence of Load Current and Separation Velocity on Arc Discharge at Breaking of Electrical Contacts," Proc. ICEC2020, pp.68-73, June 2022.

[11] A. Ishihara, J. Sekikawa, "Arc Duration and Dwell Time of Break Arcs Magnetically Blown-out in Nitrogen or Air in a 450VDC/10A Resistive Circuit," IEICE Trans. Electron., Vol. E101-C, No.9, pp.699-702, Sept. 2018.

[12] J. Sekikawa and T. Kubono, "Voltage - Current Characteristics of Breaking Arc at Constant Opening Speed in the Air," IEEE Trans. CPT, Vol. 27, no.1, pp.167-171, Mar. 2004.

[13] K. Hamamoto, J. Sekikawa, "Investigation of Time Evolution of Length of Break Arcs Occurring in a 48VDC/50-300A Resistive Circuit," IEICE Trans. Electron., Vol. E102-C, No.5, pp.424-427, May 2019.

[14] H. Yazaki, J. Sekikawa, "Dependence of Arc Duration and Contact Gap at Arc Extinction of Break Arcs Occurring in a 48VDC/10A-300A Resistive Circuit on Contact Opening Speed," IEICE Trans. Electron., Vol. E104-C, No.11, pp.656-662, Nov. 2021.

[15] R. Holm, Electric Contacts, 4th ed., Springer-Verlag, Berlin, pp.279-286, 1967.

[16] P. G. Slade, Electrical Contacts: Principles and Applications, Second Edition, pp.588-592, CRC Press, 2014.